Corrosion behavior of mild steel in glycol solution

IISER PUNE

A Dissertation thesis submitted to

Chemistry Division

Indian Institute of Science Education and Research (IISER),

Pune- 411008

Done for the partial fulfilment of the BS-MS Dual Degree Programme during the academic year 2016-17

By

N. Jocinth Selvakumar

20101088

Under the guidance of

Dr. Rakesh Chandra Barik,

Senior Scientist,

CSIR Central Electrochemical Research Institute,

Karaikudi- 630006

TITLE	PAGE

International Collaboration & Publicity Section

No.14-03-03-2016- 17- ICP

March 16, 2017

CERTIFICATE

This is to certify that this Dissertation entitled *"Corrosion Behavior of Mild Steel in Glycol Solution"* towards the partial fulfilment of the BS-MS (Chemistry) Dual Degree Programme at the Indian Institute of Science Education and Research (IISER), Pune - 411 008 represents original research carried out by **Mr. N. Jocinth Selvakumar** at CSIR-Central Electrochemical Research Institute, Karaikudi under the supervision of **Dr. Rakesh Chandra Barik, Senior Scientist,** Corrosion and Materials Protection Division during the academic year **2016 - 2017.**

16/3/17

(Dr.S.Sathiyanarayanan)
Senior Principal Scientist

प्रधान, आईसीपी अनुभाग
HEAD, ICP Section
केन्द्रीय विद्युत रसायन अनुसंधान संस्थान
Central Electrochemical Research Institute
कारैकुडी / KARAIKUDI- 630 006

DECLARATION

I hereby declare that the matter embodied in the report entitled "Corrosion behavior of mild steel in glycol solution" are the results of the investigations carried out by me at the Department of Corrosion and Material Protection, CSIR-Central Electrochemical Institute, Karaikudi under the supervision of Dr. Rakesh Chandra Barik and the same has not been submitted elsewhere for any other degree.

Rakesh Barik
30/3/2012

Dr. Rakesh Chandra Barik

Senior Scientist,

CSIR-CECRI, Karaikudi

30.03.17

N. Jocinth Selvakumar

BS-MS Student,

IISER Pune

ACKNOWLEDGEMENT

Abstract

Since glycol solutions such as ethylene glycol are hygroscopic in nature, they are used in natural gas industries to remove water by absorption before passing the gas into pipelines for distribution but the water absorbed glycol promotes corrosion in the glycol regeneration unit that is made of mild steel components. This work which was undertaken in two different perspectives, namely corrosion and oxidation, tried to understand and address real life scenarios and recreate them in lab environment. The corrosion rate of mild steel in ethylene glycol solution depends on water concentration. A diluted ethylene glycol mixture is more corrosive than a concentrated mixture. When chloride is added to the system, the corrosion rate gets enhanced. A protective surface film was observed on mild steel in 100% EG system and it got damaged when water or chloride was added to it. In cyclic voltammetry scans, when 'mirror polished' mild steel samples were used in different electrolytes (1M KOH, 0.5M EG+1M KOH and 0.5M TEG+1M KOH), there were no oxidation peaks. But, when mild steel samples were immersed in distilled water or chloride solution for 24 hours to allow the formation of oxides on their surfaces and used, there were oxidation peaks. This shows the catalytic behavior of iron oxides. Impedance study corresponds with the results of potentiodynamic technique.

LIST OF FIGURES

LIST OF TABLES

1. Introduction

Natural gas which is pumped up from underground, is considered as one of the most important energy sources in the world. It has considerable amount of water content, along with other impurities such as chloride, etc. So, it's really important to remove water content from natural gas before it is passed into pipelines for distribution (Neagu & Cursaru, 2017). Natural gas industries use 'glycol dehydration unit' to absorb water from the natural gas that is being pumped up and the glycol is also recycled back.

Even though, there are other desiccant systems that can absorb moisture, using glycols is economical. Glycols can reduce water content in the natural gas from 19.84lb/MMSCF to well below 6-7lb/MMSCF which is the tolerated level of water content in pipelines (Anyadiegwu, Kerunwa, & Oviawele, 2014). Wet gas that is pumped up from underground is passed into glycol contractor of the dehydration unit. The contractor consists of several trays that are also known as 'bubble cap trays'. The number of trays varies from 4 to 12 depending on the unit. Wet gas is passed into the chamber from the lower side of the contractor and lean glycol (glycol without any water content) is collected from the upper side of the contractor. Lean glycol runs towards the lower side through the trays. Since glycol can absorb water, when wet gas makes contact with lean glycol in the trays, the water gets removed from the gas. It passes through every tray and gets collected as dry gas from the outlet present at the top of the contractor.

The rich glycol (glycol with water content) is passed into the regeneration unit from the lower side of the contractor. Since, ethylene glycol is required in large amount inside the contractor to absorb moisture, it is economically important to regenerate ethylene glycol (AlHarooni et al., 2016). Rich glycol flows into still column through heat exchange coil. While passing through this, rich glycol gets heated up a little. From still column, the rich glycol is guided into flask tank where it is separated from hydrocarbon gases if any are present. Rich glycol flows through a filter and again into the still column. It moves into the lower side of the column and is passed into reboiler chamber. In some dehydration unit, the flash tank may not be present. In such case, rich glycol is passed into reboiler directly. Rich glycol gets heated up to the necessary temperature in the reboiler so that water gets

separated from it as water vapor. Water vapor reaches the top of the still column and gets released. Regenerated lean glycol is passed into the glycol pump through surge drum. The pressure of lean glycol is adjusted according to the contractor pressure before it reaches the glycol contractor for reuse (Anyadiegwu et al., 2014)
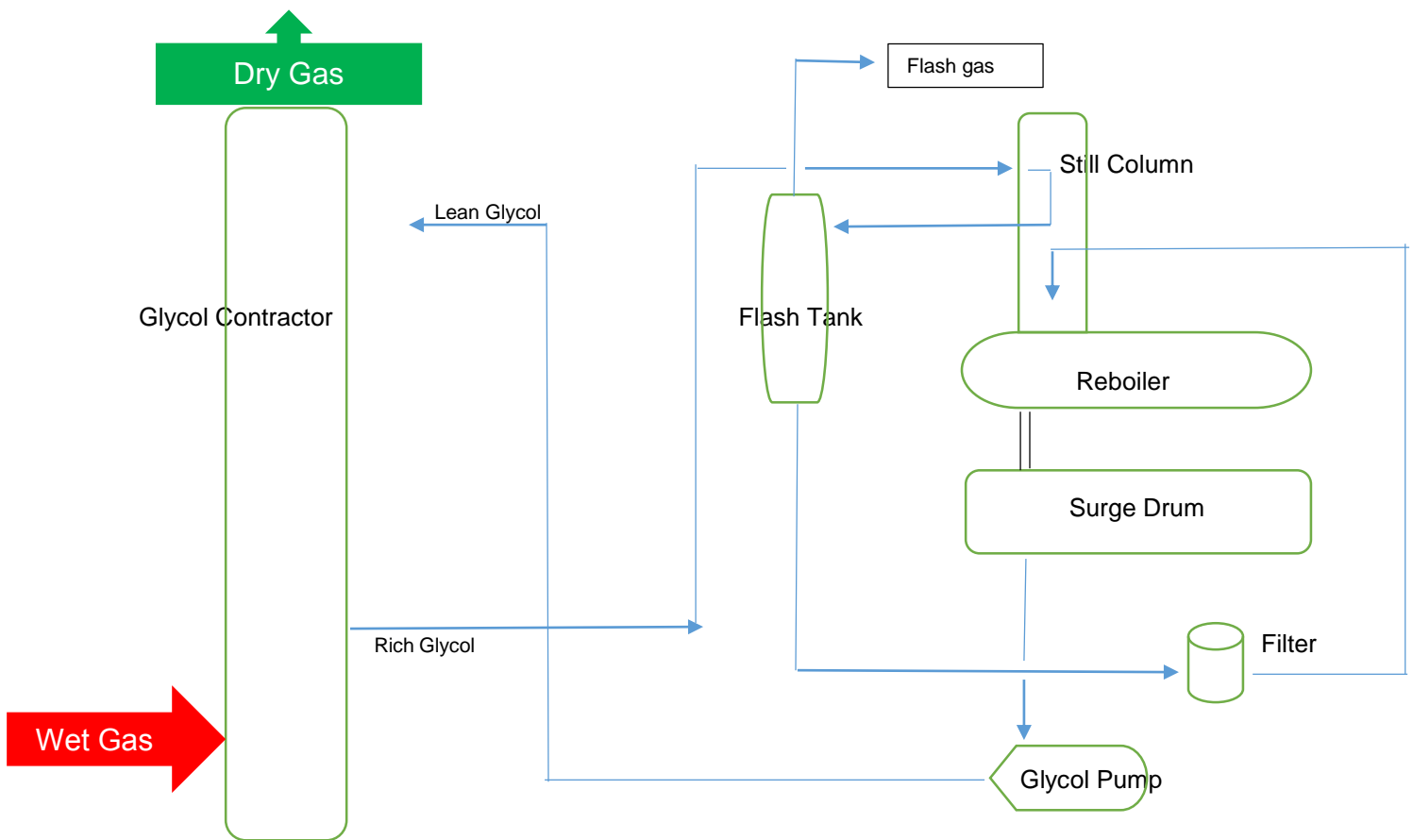
Figure 1: Flow chart of glycol dehydration unit

This research work is based on three main aspects that happen inside the dehydration unit.

1. When glycol comes out of the contractor as rich glycol, it is passed into the regeneration unit whose components are made of mild steel. This glycol-water mixture promotes corrosion in mild steel.

2. Through still column, the mixture goes into reboiler where it gets heated up to remove water. Here, glycol gets oxidized and can result in the formation of glycolic acid which, in turn, is said to cause corrosion in mild steel (Sekine, Hayakawa, Negishi, & Yuasa, 1990). The role played by iron oxides in the oxidation process is also in question.

3. When dry gas is collected from the top of the contractor, there might be some carryover of glycol into the pipeline along with the gas.

Based on these aspects, this work is divided into three categories namely corrosion, oxidation and flow behavior parts. The glycol which was used in this work is ethylene glycol $(CH_2OH)_2$. Since, glycol-water mixture promotes corrosion on mild steel, behavior of different concentrations of glycol-water mixture was investigated in corrosion part using potentiodynamic polarization technique, mass loss experiment and electrochemical impedance technique. Then, 3.5% NaCl was added to the system (The salinity of sea water is 3.5% i.e. 35g/L. This is the coarse saline level) and results were correlated (Sekunowo, Adeosun, & Lawal, 2013). Using Scanning Electron Microscope (SEM), surface morphology of mild steel samples at different conditions were observed. All these experiments are done in static condition. But, since there might be some carryover of glycol into the pipelines, it is necessary to discuss mild steel corrosion in flow environment. This was done using rotating cylinder electrode (RCE). Using the same technique, mass transfer kinetics of cathodic reactants was also investigated.

'Where there is machine, there will be corrosion'. Every year, industries dealing with machinery are spending millions on corrosion. Lot of works were done and are going on and will be done on corrosion since there are no ways to prevent corrosion but ways to minimize it. There are works that tried to address mild steel corrosion through gravimetric analysis and through polarization techniques (Khadiri et al., 2015). Usually, the polarization works in mild steel are not directly related to corrosion in natural gas industries. When it comes to electro-oxidation of ethylene glycol, there are works with different electrodes (Chen, Zhu, Yang, Pi, & Cui, 2011) but, no literature was found with mild steel. There are works that tried to create thermodynamic modelling of natural gas dehydration using glycols (Gironi, Maschietti, & Piemonte, 2010) and mathematical modelling of internal corrosion but their long range validity is questionable. But, this work tries to mimic what's happening in glycol dehydration unit by combining polarization and electro-oxidation techniques and address the questions of glycol corrosion.

2. Materials and Methods

2.1) Materials

Mild steel for the study was supplied by Alfa Aesar, United Kingdom. Ethylene glycol, triethylene glycol, sodium chloride, Fe_2O_3, Fe_3O_4 were supplied by Sigma Aldrich, Bangalore. Electrolytes were prepared using ultrapure distilled water and 3.5% NaCl. The mild steel samples were mechanically polished to mirror finish using polishing machine, different grades of SiC papers, diamond paste. They were degreased using acetone, rinsed in distilled water and were dried in desiccators. The chemical composition of mild steel is C: 0.24%, Pb: 0.04%, S: 0.045%, N: 0.009% and Fe: rest.

2.2) Infrared Measurements

Fourier transform infrared spectroscopy (FTIR) was performed in the transmittance mode by using model Nexus 670 with Centaurms 10x microscope having spectral range 4000 to 375 cm^{-1}, spectral resolution 0.125 cm^{-1} with a MCT-A detector.

2.3) SEM Characterization

The morphology of the sample surfaces were examined by scanning electron microscope (SEM) (Hitachi S-3000H, Japan) in secondary electron mode at accelerating voltage of 25 KV.

2.4) Gravimetric Mass Loss

Gravimetric assessments were carried out to quantify the influence of water content and chloride (3.5% NaCl) on corrosion of mild steel in ethylene glycol with different concentrations. The surface preparation of mild steel samples involved various grades of SiC papers and with diamond paste to get mirror finish and degreased with acetone using an ultrasonicator for 10 minutes. The mirror-polished samples of dimensions (2.5× 2.5× 0.5 cm^2) were used for the gravimetric study. The samples were immersed for 240 hours in ethylene glycol-water mixture and ethylene glycol-chloride mixture (3.5% NaCl) separately as two sets of experiments. The initial and final weights of the mild steel samples were measured by a digital weighing balance SHIMAZDU AUW220D (0.01 mg).

The gravimetric mass loss was converted to corrosion rate (CR) in mm/year through equation (1) (Kina & Ponciano, 2013).

$$CR = \frac{87.6\ W}{\rho AT} \qquad (1)$$

Where,

CR = Corrosion rate (mm/year)

W = Weight loss (mg)

ρ = Density (g/cm^3)

A = Area (cm^2)

T = Time (hour)

2.5) Electrochemical Measurements

Electrochemical experiments were run using 'Metrohm Autolab' potentiostat instrument.

2.5.1) Potentiodynamic Polarization

The electrochemical study was carried out on mild steel (1 cm^2) in ethylene glycol electrolyte with variation of water content. Also, the same was done with varied concentration of 3.5% NaCl. This was a 'three electrode cell' experiment. The voltage was measured by saturated calomel reference electrode whose potential is fixed (0.242 V vs. NHE). The current passage was measured between the working electrode (mild steel) and the counter electrode (platinum). Mild steel sample (working electrode) was prepared like it was done in gravimetric experiment. Open circuit potential (OCP) was measured for 1800 seconds.

2.5.2) Cyclic Voltammetry

This electrochemical study was carried out for the oxidation part. The setup was same as the potentiodynamic experiment. In this experiment, KOH was added to the electrolyte so that pH of the electrolyte was increased. This, in turn, would increase the concentration of OH$^-$ ions in the electrolyte which results in the de-protonation of alcohol and lowers the energy barrier of oxidation reaction (Kwon, Lai, Rodriguez, & Koper, 2011). The electrolytes that were used for this experiment were 0.5 M ethylene glycol+1 M KOH, 0.5

M triethylene glycol+1 M KOH and 0.5 M glycolic acid+1 M KOH (Xin, Zhang, Qi, Chadderdon, & Li, 2012)

2.5.3) Rotating Cylinder Electrode
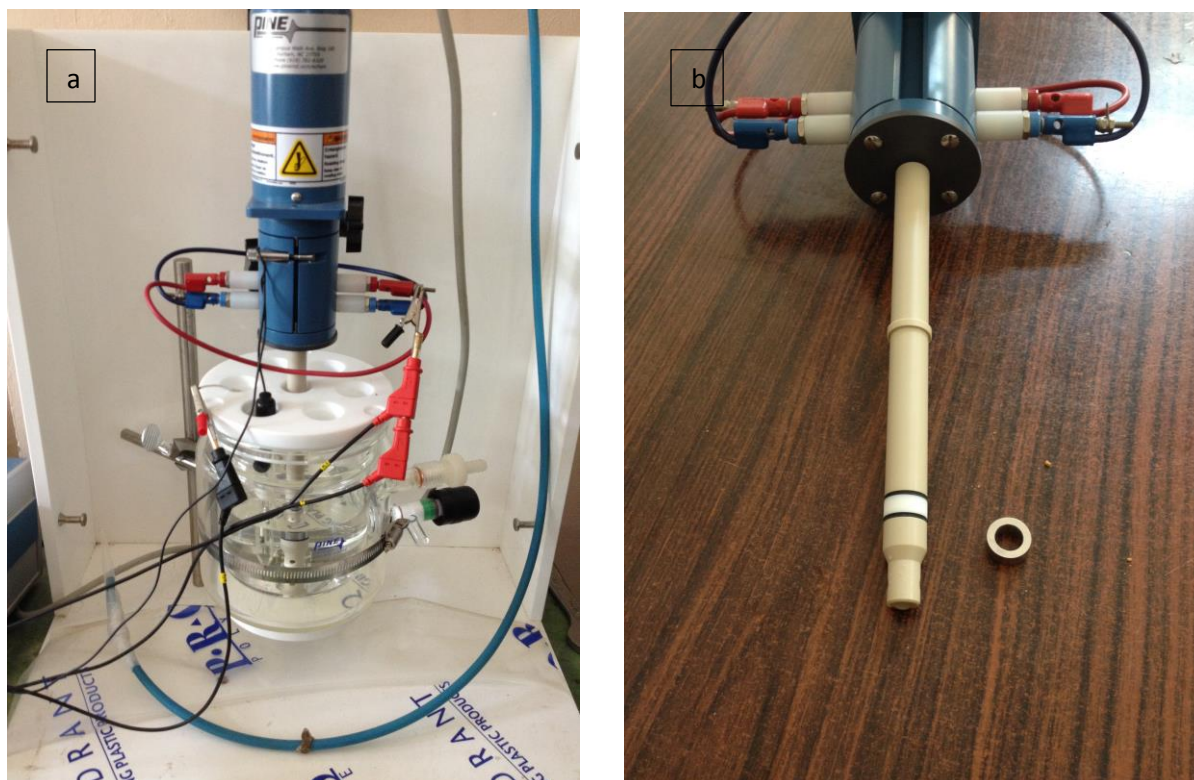
Figure 2: Images of (a) rotating cylinder electrode (RCE) and (b) rotating shaft and mild steel sample.

Using rotating cylinder electrode, flow environment (pipeline environment) was created inside the cell. The rotating shaft was attached with a motor to its top. Mild steel sample which is ring shaped was fit onto the shaft and the rotation rate was controlled using a controller setup. Rotation rate could be varied from 10 rpm to 4000 rpm. Through linear sweep voltammetry (LSV) electrochemical technique, graphs were obtained for different

rpms and different conditions. Electrolytes that were used for this experiment were 600 ml of different concentrations of ethylene glycol-water mixture and ethylene glycol-3.5% NaCl mixture.

2.5.3.1) Linear sweep voltammetry (LSV)

In LSV, current is measure against potential and there will be a linear relationship between potential and time. Ring shaped mild steel sample, saturated calomel electrode and platinum electrode were used as working, reference and counter electrodes respectively. OCP was measured for 1800 seconds.

2.5.3.5) Electrochemical impedance spectroscopy (EIS)

EIS measurements were run FRA impedance in Autolab. The experimental setup was same as the potentiodynamic polarization technique. OCP was determined for 1800 seconds. The frequency range was from 0.01 Hz to 100 kHz with an AC wave of 10 mV. The graphs obtained were done nonlinear least square fitting using Zswimpwin program by Autolab (Rajendran, Vinoth, Shanthi, Barik, & Pattanayak, 2014) (Gopi et al., 2014).

Electrochemical experiments	OCP determination (s)	Start potential (V)	Stop potential (V)	Scan rate (V/s)	Upper vertex potential (V)	Lower vertex potential (V)	No. of stop crossings
Linear/potentiodynamic polarization	1800	-1.00	+1.00	0.001	-	-	-
Cyclic voltammetry	-	0.00	0.00	0.010	+1.00	-1.00	10
Linear sweep voltammetry	1800	0.00	-1.00	0.010	-	-	-
FRA impedance	1800	-	-	-	-	-	-

Table 1: Staircase values for different electrochemical techniques in NOVA software using 'Metrohm Autolab' potentiostat instrument.

3. Results and Discussions

3.1) pH measurements
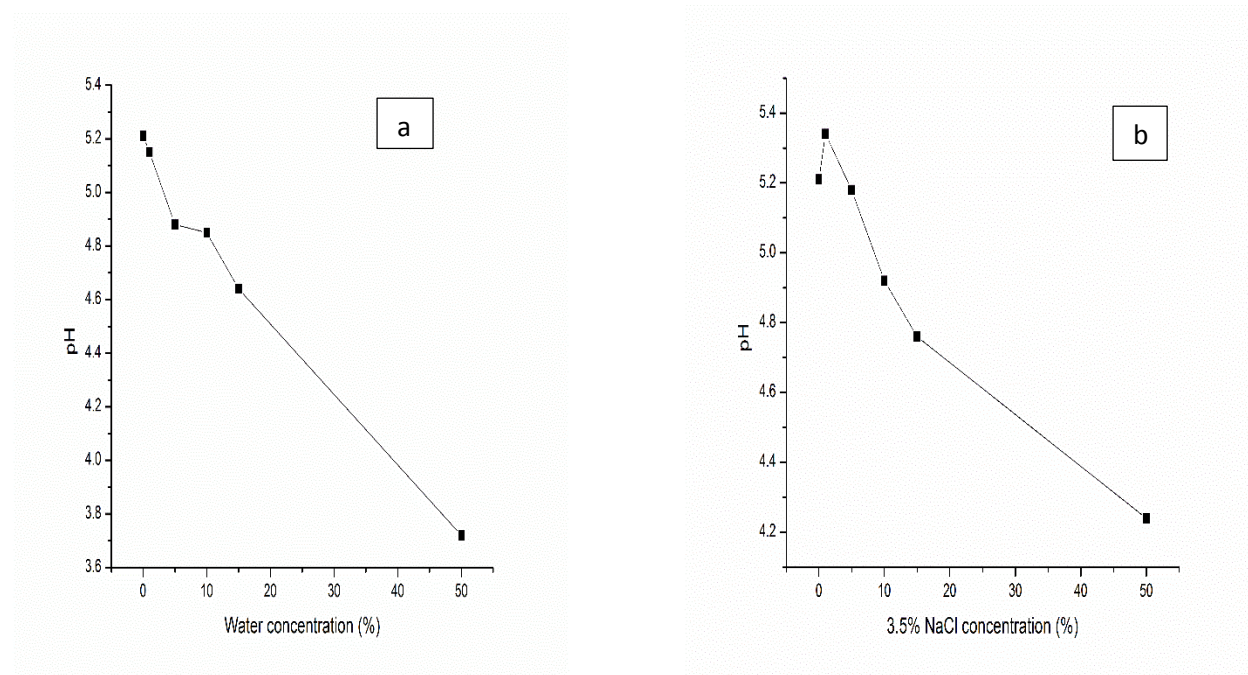
Figure 3: pH measurements of different concentrations of (a) EG-water mixture and (b) EG-3.5% NaCl mixture.

Different concentrations of ethylene glycol-water mixture and EG-3.5% NaCl mixture were prepared and pH was measured for each concentration. These measurements were repeated several times to establish concurrnet validity. In figure 3a, with increasing water concentration, pH of EG-water mixture was dropping. From pH ~5.2 at 0% water concentration, it reached pH ~3.7 at 50% water concentration. In figure 3b, pH increased slightly when concentration of 3.5% NaCl was increased from 0 to 1 (pH at 0% was ~5.2 and pH at 1% was ~5.3). But, when the concentration was increased to 5%, the pH started to drop and reached ~4.2 at 50% of 3.5% NaCl. In both the cases, eventhough pH values were close at concentration from 0 to 10%, there was a fall in pH when water/3.5% Nacl concentration was increased. When the concentration was increased to 50%, a drastic fall in pH values was observed.

3.2) Finding corrosion rate using mass loss experiment
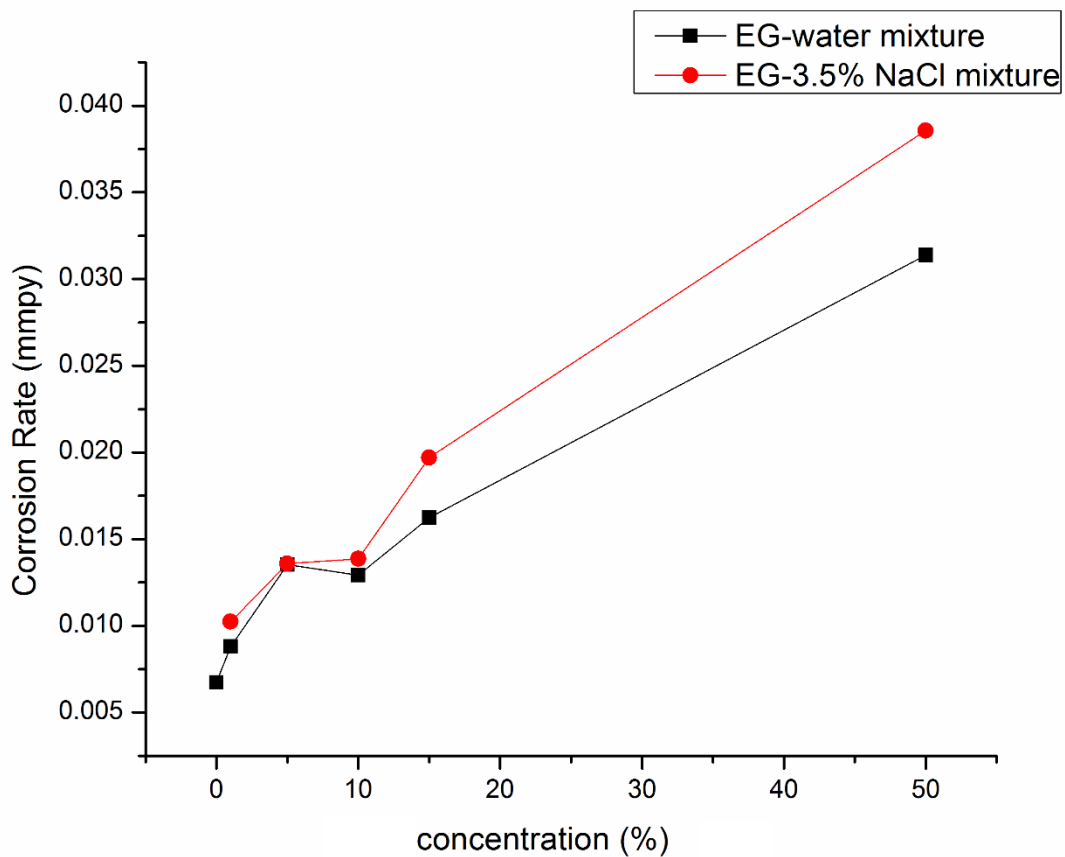
Figure 4: Graph represents corrosion rate vs. different concentrations of EG-water mixture and EG-3.5% NaCl mixture.

Mirror polished mild steel samples were immersed in different concentrations of EG-water mixture for 120 hours. The same experiment was done EG-3.5% NaCl mixture too. The concentrations of EG used for these experiments were 100%, 99%, 95%, 90%, 85% and 50%. Using equation (1), corrosion rate (CR) in mmpy for each concentration was calculated (Density, ρ = 7.6 g/cm^3 ; Area, A = 2.5 cm^2 ; Time, t = 120 h). In figure 4, when

water/3.5% NaCl concentration was increased, corrosion rate increased. Thus, corrosion rate is directly proportional to water/3.5% NaCl concentration.

3.3) SEM Analysis
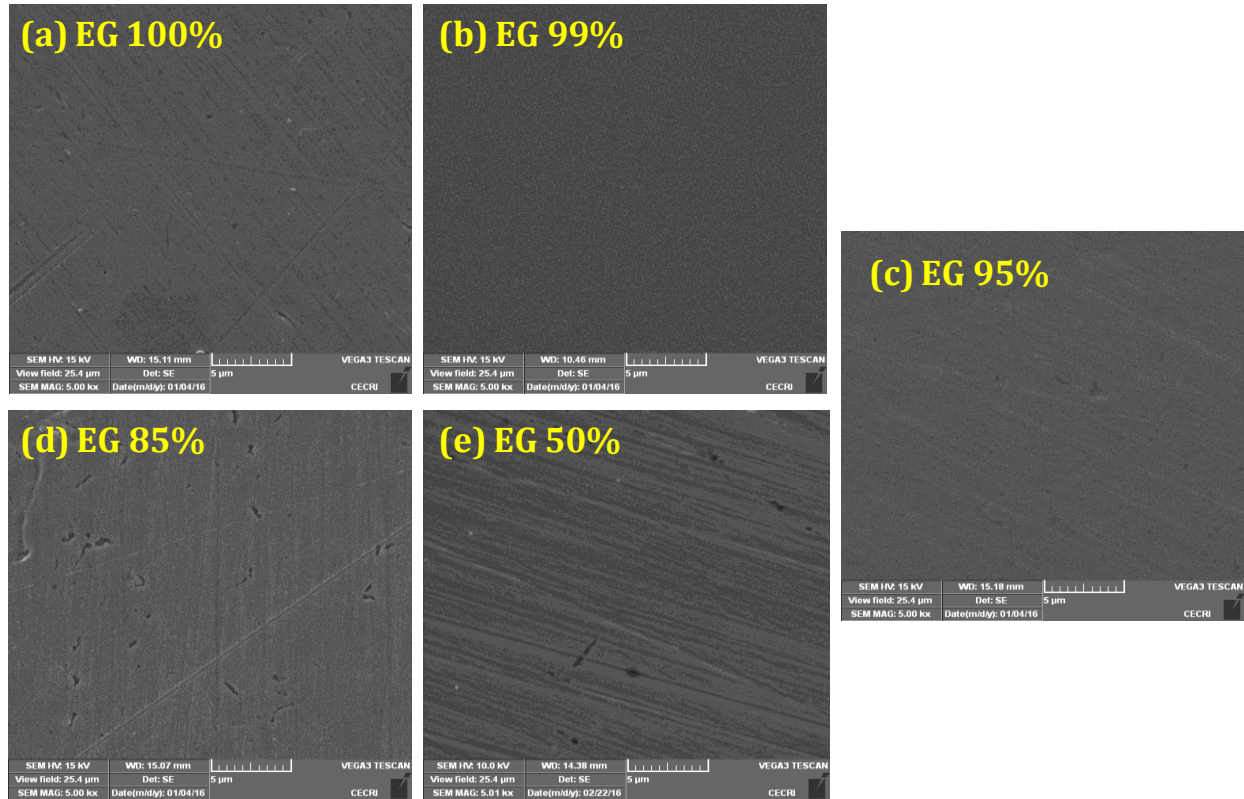
Figure 5: SEM images of mild steel samples immersed in different concentrations of EG-water mixture.
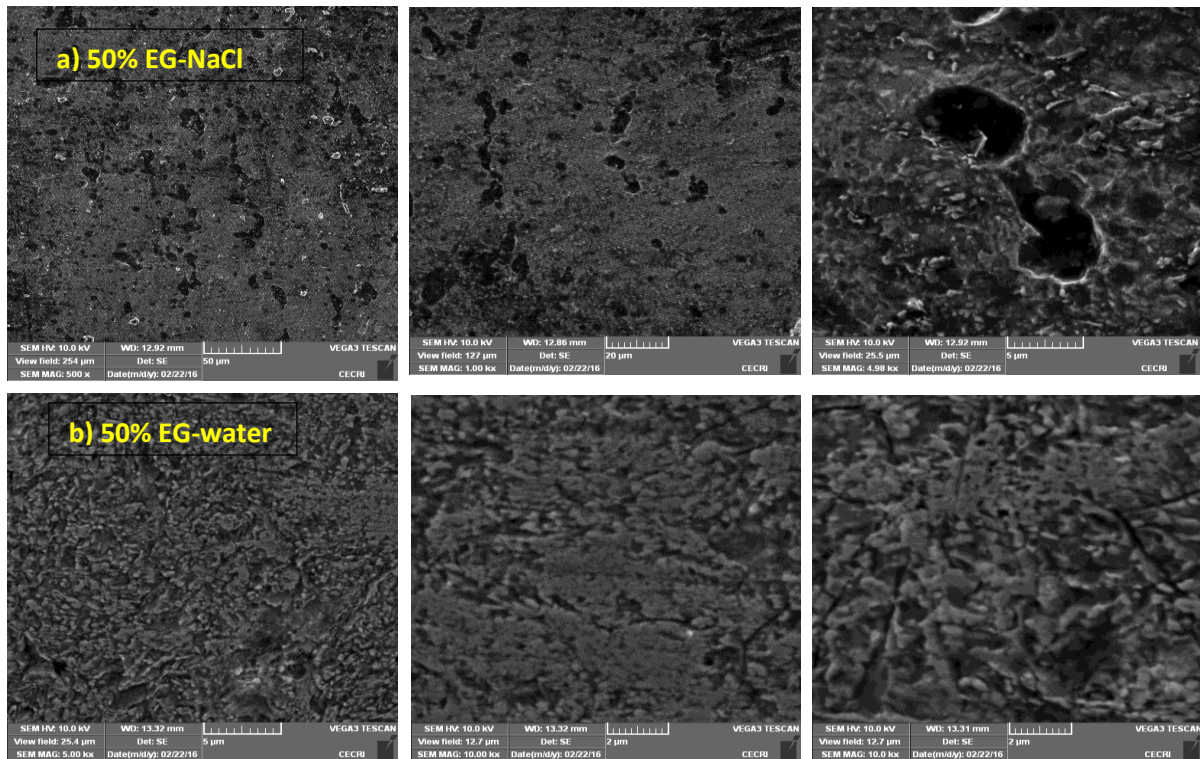
Figure 6: Magnified images of mild steel samples in (a) 50% EG-NaCl and (b) 50% EG-water mixtures after cleaned with Clarke's solution.

Mild steel samples immersed in different concentrations of EG-water mixture were analyzed under scanning electron microscope. Figure 5 shows that an adsorption film was formed on the surface of mild steel sample in 100% EG system. When water concentration was increased, the film on the mild steel sample was disrupted and the surface got damaged. Mild steel samples of 50% EG-water and 50% EG-3.5% NaCl systems were cleaned using Clark solution which is a combination of hydrochloric acid, stannous chloride and antimony trioxide (Kina & Ponciano, 2013). In figure 6b, on cleaning the surface with Clark solution, mild steel sample in 50% EG-water mixture showed a roughened surface. But, in figure 6a, mild steel sample showed pitting formation because of the presence of chloride in the system.

3.4) Potentiodynamic polarization of EG-water and EG-3.5% NaCl mixtures

Figure 7: Polarization graph of ethylene glycol-water mixture
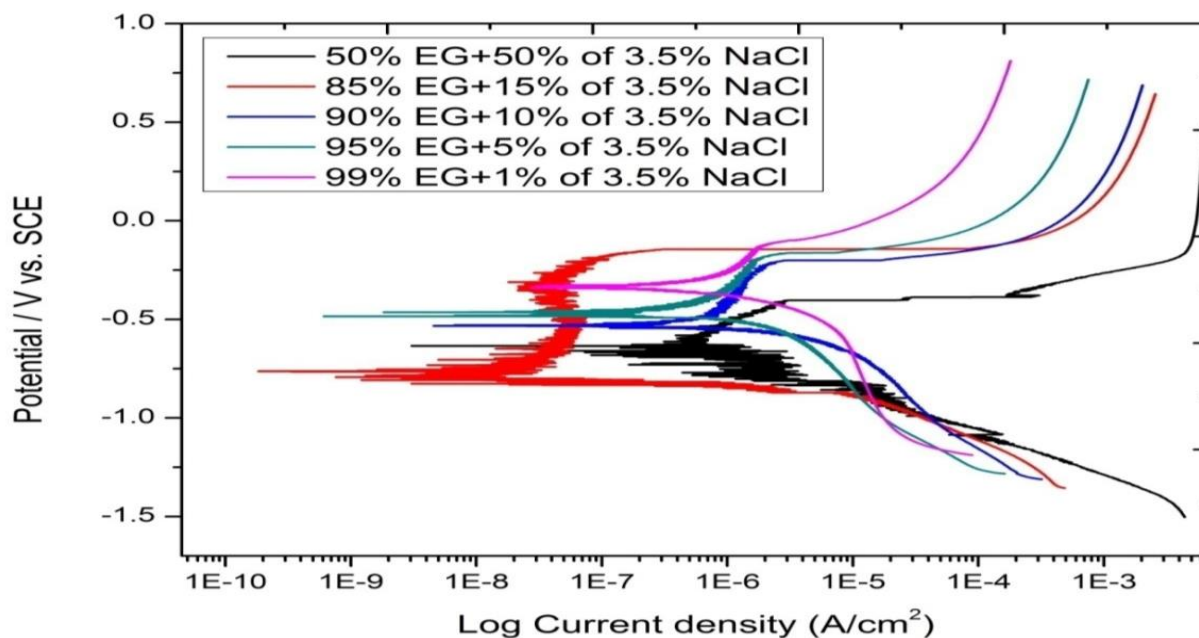
Figure 8: Polarization graph of ethylene glycol-3.5% NaCl mixture

In figure 7, as the water concentration was increased, the anodic and cathodic curves shifted towards more negative potential. And, the current density increased with the increased concentration of water. EG-3.5% NaCl mixture also followed a similar pattern as shown in figure 8

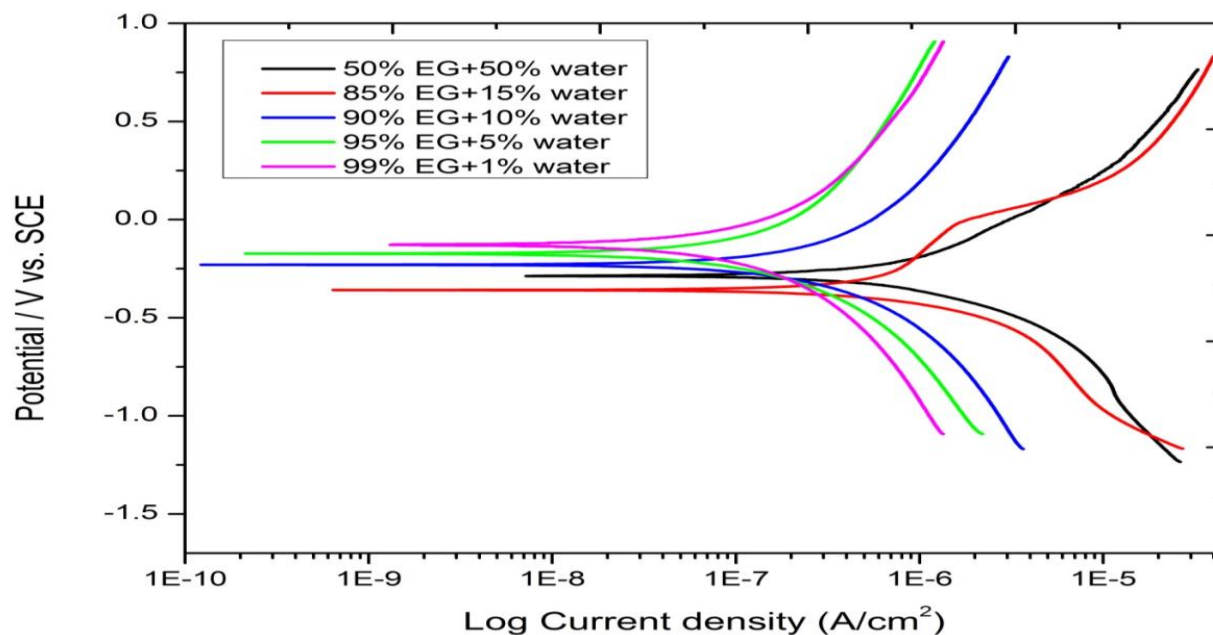| EG-water mixture			EG-3.5% NaCl mixture		
Water content (%)	E$corr$ (V / SCE)	i$corr$ ($\mu A\ cm^{-2}$)	Chloride content (%)	E$corr$ (V / SCE)	i$corr$ ($\mu A\ cm^{-2}$)
1	-0.125	0.046	1	-0.329	0.582
5	-0.173	0.056	5	-0.484	0.773
10	-0.229	0.117	10	-0.532	0.901
15	-0.358	0.638	15	-0.765	0.106
50	-0.287	0.658	50	-0.634	2.210

Table 2: Polarization data for mild steel in ethylene glycol- water mixture and ethylene glycol-3.5% NaCl mixture.

E$corr$ and i$corr$ values for both set of experiments were given in table 2. These values were calculated by taking the slopes of anodic and cathodic curves (Schwerdtfeger, 1957). The intersection point (x, y) of both the slopes will be (i$corr$, E$corr$). With the increase in water/chloride concentration, i$corr$ values increased. In EG-water system, i$corr$ values at 1% and 50% water concentrations were 0.046 $\mu A\ cm^{-2}$ and 0.658 $\mu A\ cm^{-2}$ respectively. And, in EG-3.5% NaCl system, i$corr$ values at 1% and 50% chloride concentrations were 0.582 $\mu A\ cm^{-2}$ and 2.210 $\mu A\ cm^{-2}$ respectively. The increase in i$corr$ values directly corresponds to increased corrosion rate. i$corr$ values of different concentrations in EG-3.5% NaCl mixture were pretty high when compared with the

respective concentrations in EG-water mixture. This, again, showed that corrosion rate would increase if chloride was added to the system in electrochemical point of view.

3.5) Oxidation of ethylene glycol

3.5.1) Heating

10 ml of EG was heated as two different experiments in presence of 0.5 g of Fe_2O_3 and 0.5 g of Fe_3O_4 respectively with constant supply of O_2 for 8 hours per day.
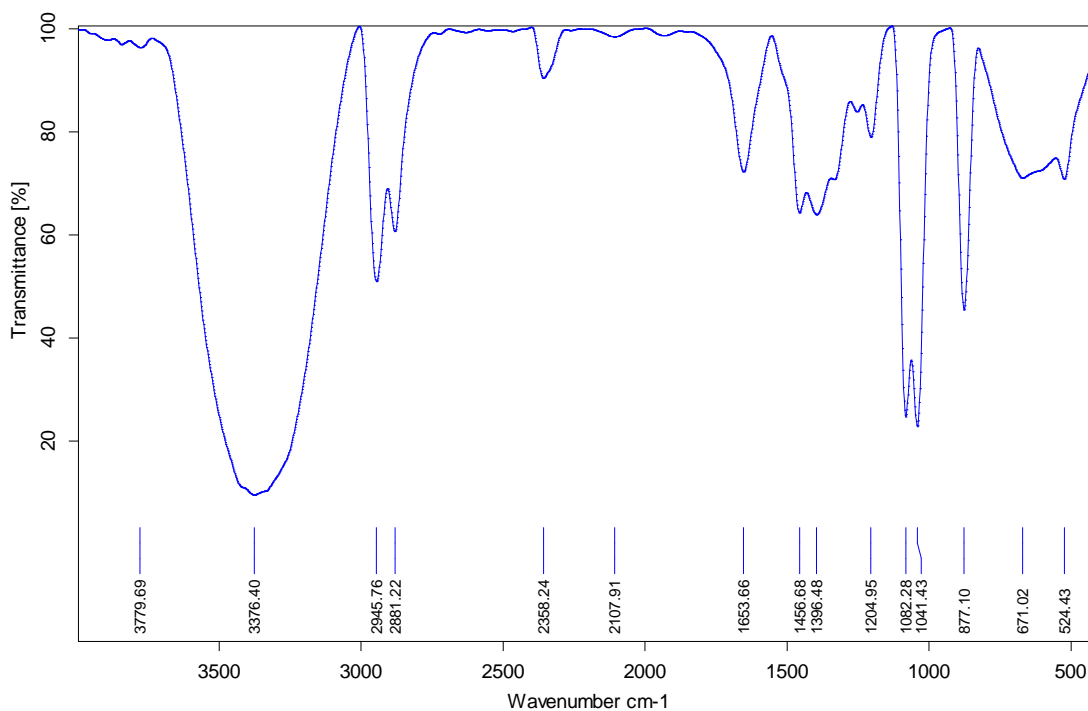
Figure 9: IR spectrum of ethylene glycol
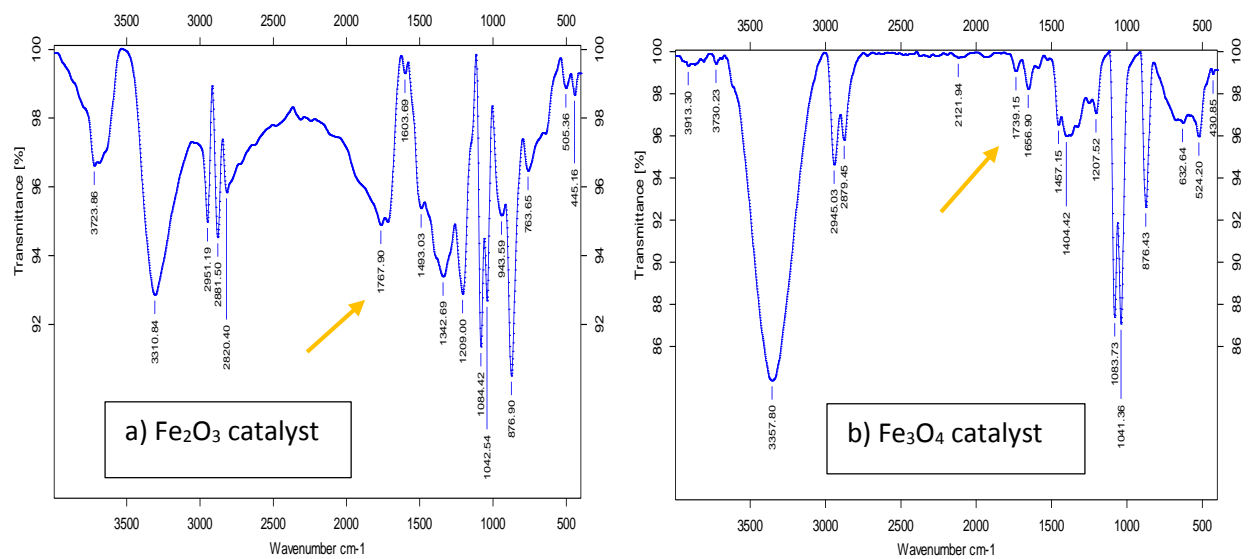
Figure 10: IR spectra of (a) heating of EG with Fe_2O_3 and (b) heating of EG with Fe_3O_4

Each day, samples (0.1 ml) were collected from both the reactions and analyzed. The results were analyzed with IR spectrum of ethylene glycol (figure 9). The samples from 5th day were analyzed and compared with figure 9. There was a peak at 1767.90 cm^{-1} for the sample with Fe_2O_3 and a peak at 1739.15 cm^{-1} for the sample with Fe_3O_4. This confirmed that traces of acid group were present in the samples which in turn confirmed the oxidation of ethylene glycol. The same experiment was run without any catalyst for 9 days and no acid peak was seen. This shows the catalytic behavior of iron oxides on oxidation of ethylene glycol.

3.5.2) Cyclic voltammetry scans
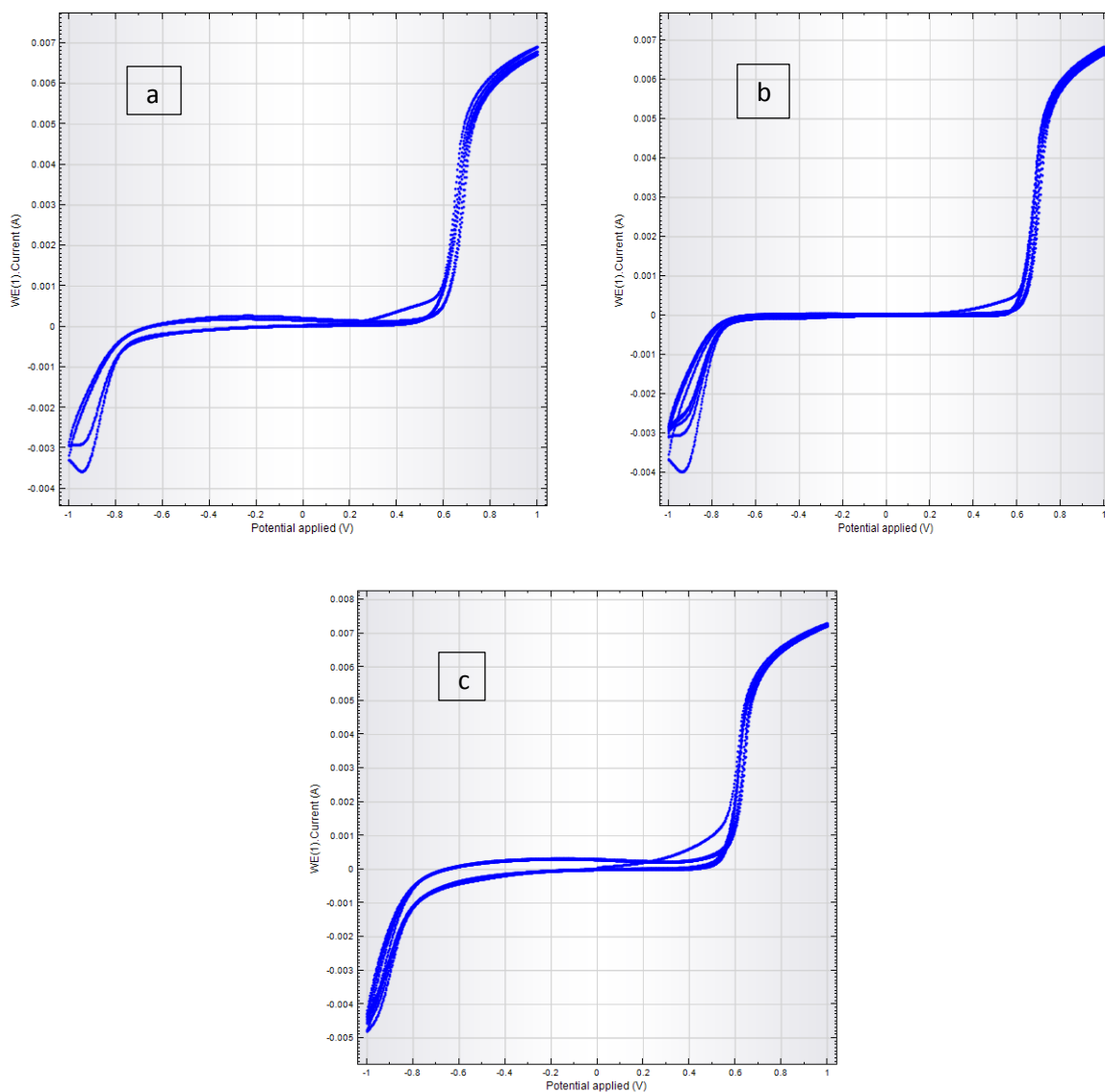
Figure 11: CV Scans of (a) 0.5M EG+1M KOH, (b) 0.5M TEG+1M KOH and (c) 1M KOH with mirror polished mild steel sample as working electrode.

In figures 11a and 11b, when CV scans were run in 0.5M EG+1M KOH and 0.5M TEG+1M KOH electrolytes with mirror polished mild steel samples as working electrodes, there were no oxidation peaks. To confirm further, only 1M KOH was taken as electrolyte and CV scans were run. There were no oxidation peaks (figure 11c). This shows that mirror polished mild steel is not catalytically active.
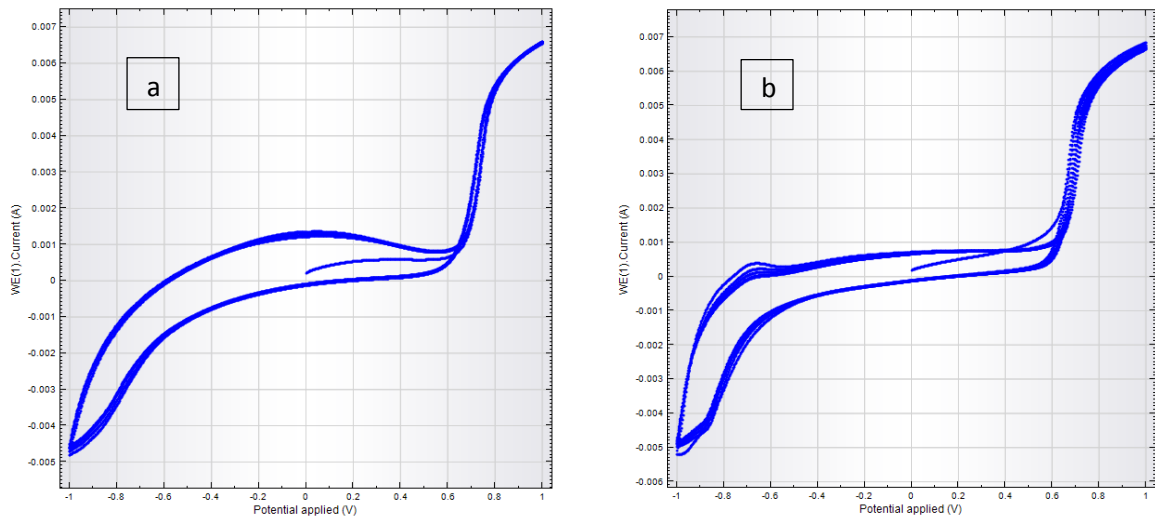
Figure 12: CV scans of (a) 0.5M EG+1M KOH and (b) 0.5M TEG+1M KOH with modified mild steel sample using distilled water as working electrode
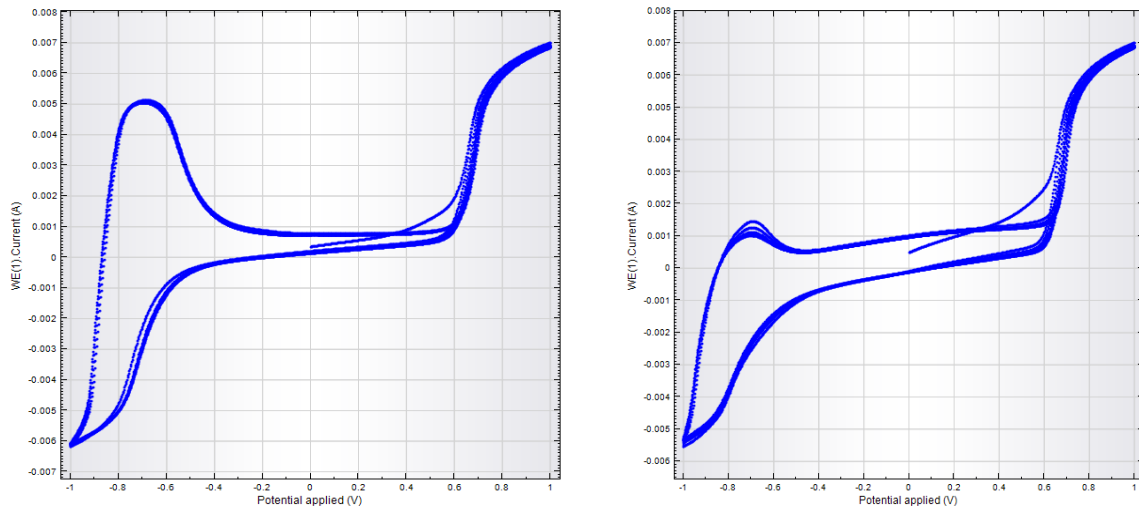
Figure 13: CV scans of (a) 0.5M EG+1M KOH and (b) 0.5M TEG+1M KOH with modified mild steel sample using 3.5% NaCl

In figure 12a, when mild steel which was modified by immersing in distilled water for 24 hours to allow the formation of oxides on its surface and used in 0.5M EG+1M KOH, there

was a little or no oxidation. When mild steel which was modified using distilled water was used in 0.5M TEG+1M KOH, there was mild oxidation (figure 12b).

In figures 13a and 13b, mild steel immersed in 3.5% NaCl showed good oxidation peak in 0.5M EG+1M KOH and 0.5M TEG+1M KOH. This, again, demonstrates the aggressiveness of chloride ions. When we compare figures 11, 12 and 13, mild steel with iron oxides on its surface showed oxidation as opposed to mirror polished mild steel. This proves the catalytic behavior of iron oxide through electrochemical technique.

3.6) EIS measurements using FRA impedance
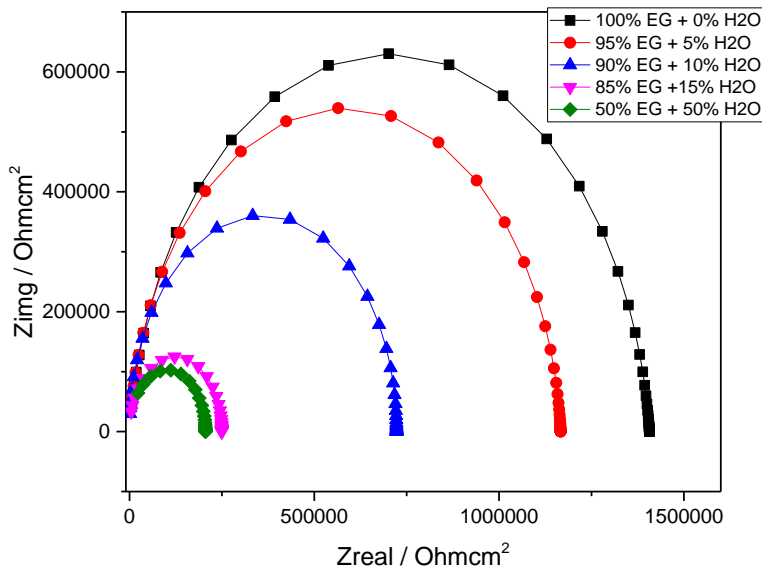
Figure 14: Impedance plots (Nyquist curve) of mild steel in different concentrations of EG-water mixture
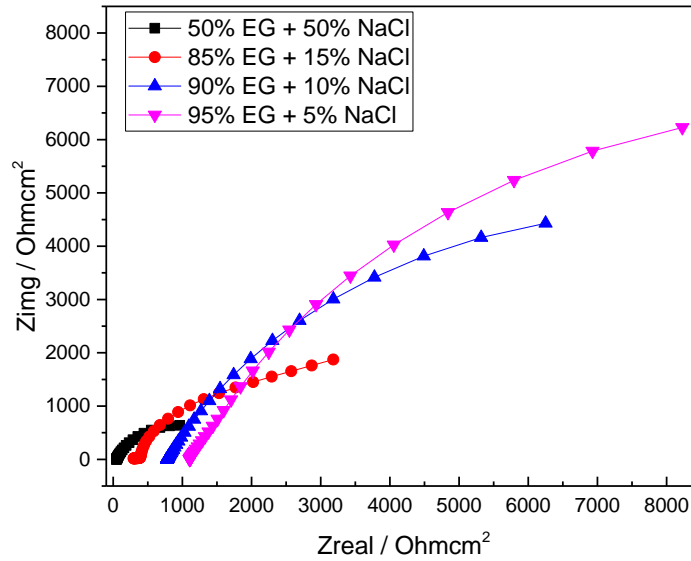
Figure 15: Impedance plots (Nyquist curve) of mild steel in different concentrations of EG-3.5% NaCl mixture

In figure 14, the frequency intercept in the real axis was high which is due to solution resistance, R_s (Rajendran et al., 2014). Since icorr is inversely proportional to resistance(Silverman & Carrico, 1988), when there is high resistance, icorr will be low. This, in turn, will show low corrosion rate because corrosion rate is directly proportional to icorr (Kina & Ponciano, 2013). In lower water concentrations, ethylene glycol acted as an inhibitor on mild steel with high polarization resistance. When water concentration was increased, the resistance reduced. When chloride was added into the system, the polarization resistance dropped significantly which accounted for high corrosion rate (figure 15).

Impedance of CPE (constant phase element) and total circuit impedance can be calculated using equations (2) and (3) respectively (Rajendran et al., 2014).

$$Z_{CPE} = \frac{1}{Q\,(j\omega)^n} = \frac{1}{Q\omega^n}\left[\cos(n\pi/2) - j\sin(n\pi/2)\right] \qquad (2)$$

(where ω = angular frequency, j = imaginary number, Q = admittance constant,

n (0<n<1) = empirical constant)

$$Z = Rs + \left[j\omega CPE + \frac{1}{Rpore + \frac{Rct}{jw\,Rct\,Cdl}} \right]^{-1} \qquad (3)$$

(where R_s = solution resistance, R_{ct} = charge transfer resistance, R_{pore} = pore resistance and C_{dl} = double layer resistance)

Samples	R_s (ohm cm^2)	CPE Ohm s^n cm^2	Frequency power (0<n<1)	R_{pore} (ohm cm^2)	C_{dl} (F cm^{-2})	R_{ct} (Ohm cm^2)
50%EG + 50% H$_2$O	0.04	8.687E-7	0.6	0.01	0.1408	1.407E6
85%EG + 15% H$_2$O	0.01	5.215E-11	0.6	0.01	9.745E7	1.167E6
90%EG + 10% H$_2$O	0.01217	2.196E-11	0.8	0.01	9.745E9	2.054E6
95%EG + 5% H$_2$O	0.01	4.707E-11	0.8	2.496E5	9.745E7	9.745E9
100%EG + 0% H$_2$O	76.98	1.172E-10	0.8	1E16	6.5E-6	2.176E13

Table 3: Impedance data for mild steel in different concentrations of EG-water mixture

Samples	R_s (ohm cm^2)	CPE (ohm s^n cm^2)	Frequency power (0<n<1)	R_{pore} (ohm cm^2)	C_{dl} (F cm^{-2})	R_{ct} (ohm cm^{-2})
50%EG + 50% 3.5%NaCl	46.56	0.000744	0.8	90.49	4.661E-5	1752
85%EG + 15% 3.5% NaCl	778.1	0.0001377	0.8	1.343E4	1.488E-5	9540
90%EG + 10% 3.5% NaCl	1105	0.0001018	0.8	6117	1.119E-5	13900
95%EG + 5% NaCl	247.3	0.000308	0.69	197.6	5.752E-5	1.456E12

Table 4: Impedance data for mild steel in different concentrations of EG-3.5% NaCl mixture.

In table 3 and 4, fit parameter values that were obtained from figures 14 and 15 are listed. In table 3, when water concentration was increased, the charge transfer resistance, R_{ct} decreased. A similar pattern was absorbed in chloride system (table 4). But, when R_{ct} values of both the systems were compared, chloride system showed very low R_{ct} values. In table 3, the high values of R_{ct} attribute to the availability of low metal area because of formation of protective film by the adsorbed glycol on the metal surface in low concentrations of water. But, in chloride system, the adsorbed layer of EG easily gets broken and chloride ions reach the metal surface even in lower concentrations. That's why the R_{ct} values are very low which attribute to high corrosion rate. These results correspond with potentiodynamic and mass loss results.

3.7) Cathodic polarization in flow conditions using rotating cylinder electrode

Using rotating cylinder electrode, flow environment was created using different rpms from 20 to 2,000. The flow is determined laminar or turbulent based on Reynold's number. When Reynold's number is more than 200, the flow is turbulent. Reynold's number is given by equation (4)

$$R_e = U_{cyl} \, d_{cyl} \, \rho \, /\mu \qquad\qquad (4)$$

(ρ = solution density (g/cm³), μ = absolute viscosity of the solution (g/cm), U_{cyl} = linear velocity (cm/s), d_{cyl} = diameter of RCE (cm))

The angular rotation, ω and linear velocity, U_{cyl} are given by equations (5) and (6)

$$\omega = 2\pi F/60 \qquad\qquad (5)$$

(where F is rotation rate)

$$U_{cyl} = \pi d_{cyl} F / 60 \qquad\qquad (6)$$

rpm	Rotation rate (rad/sec)	Linear Velocity cm/sec	Linear Velocity m/sec	Reynolds Number	Nature of flow
20	2.093	1.57	0.0157	252	turbulent
50	5.233	3.93	0.0393	631	turbulent
100	10.466	7.85	0.0785	1262	turbulent
200	20.933	15.7	0.157	2524	turbulent
500	52.333	39.25	0.3925	6310	turbulent

| 1000 | 104.666 | 78.5 | 0.785 | 12620 | turbulent |
| 2000 | 209.333 | 157 | 1.57 | 25241 | turbulent |

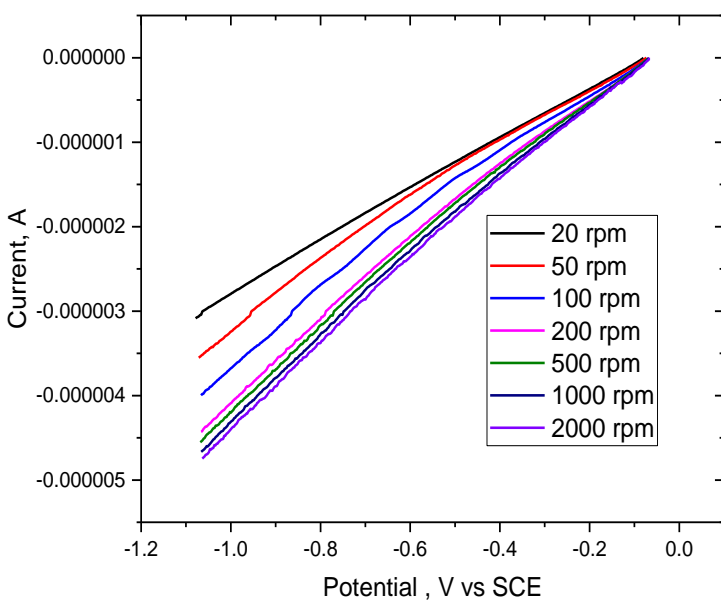**Table 5:** Calculations for rotating cylinder electrode in 3.5% NaCl solution

Figure 16: Cathodic polarization curves for oxygen reduction in 50% EG-50% water at rotating rates ranging from 20 to 2000 rpm.
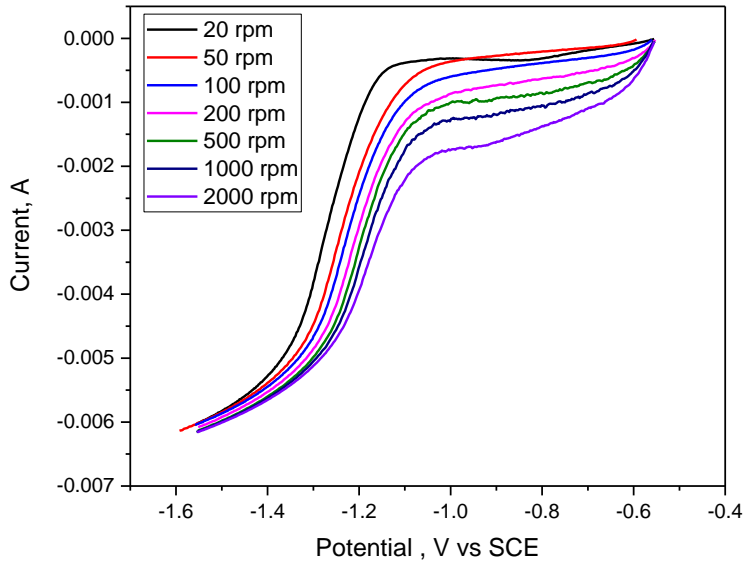
Figure 17: Cathodic polarization curves for oxygen reduction in 50% EG-50% of 3.5% NaCl at rotating rates ranging from 20 to 2000 rpm.

The LSV reactions were run at a potential range from 0 to -1 which is the cathodic range. Cathodic reactions are considered as the rate determining step of the overall electrochemical reactions. Oxygen reduction is the predominant cathodic reaction in water or O_2 environment (Santambrogio, Perrucci, Trueba, Trasatti, & Casaletto, 2015)

In figure 16, when rpm was increased from 20 to 2000 in water medium, current increased. But, there was no limiting current where current remains almost constant for a particular range of V. In figure 17, from -0.6 V to -0.95, the current was almost constant. So, limiting current can be calculated from chloride medium. This is the limiting current at which the oxidation reduction is under mass transport/diffusion control (Khan, Shanthi, Babu, Muralidharan, & Barik, 2015).

3.7.1) Limiting current vs Rotation rate

Limiting current is given by equation (7)

$$I_L = 0.0487\ z\ FAd_{cyl}^{-0.3}D^{0.644}v^{-0.344}\ C_b\omega^{0.7} \qquad (7)$$

(where z = number of electrons, F = Faraday constant, C_b = bulk concentration, D = diffusion coefficient, v = kinematic viscosity)
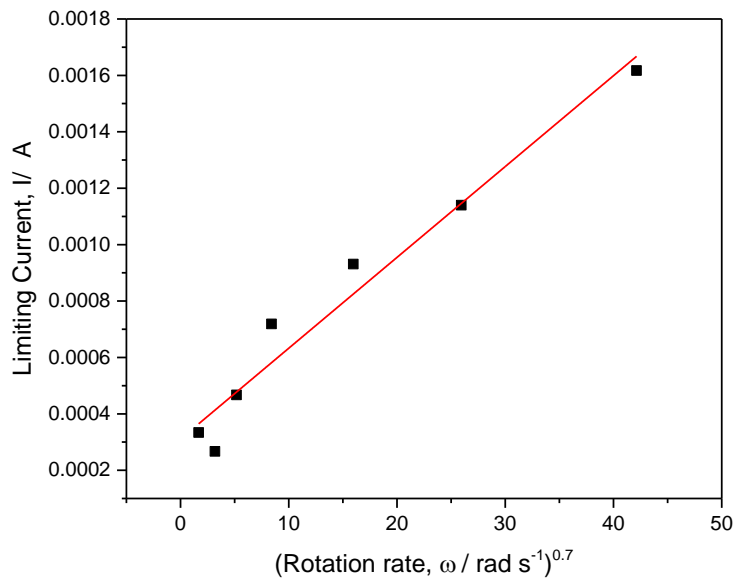
Figure 18: Limiting current *vs* rotation rate plot for the oxygen reduction reaction at the mild steel rotating cylinder electrode using ethylene glycol with 3.5 % NaCl solution

In figure 18, rotation rate and limiting current shows linear relationship even though there are some slight deviations.

From slope K of figure 18, the diffusion coefficient D, can be calculated using equation (8).

$$D^{0.644} = [K]\ /\ 0.0487\ z\ FAv^{-0.344}\ C_b \qquad (8)$$

From equation (8), the diffusion coefficient of dissolved oxygen is given by

$$D = \sqrt{|K|} \diagup 0.0487 \, z \, FA \, v^{-0.344} \, C_b \qquad\qquad (9)$$

The bulk concentration of oxygen is held constant by saturation of the chloride electrolyte to achieve a saturated concentration (C_b= 2.63 x 10^{-7} mol cm^{-3}) at 25°C. So the diffusion coefficient of oxygen is

$$D(O_2) = \sqrt{\left(\frac{|3.22 \times 10^{-5} \, A \, rad^{0.7} \, s^{0.7}|}{(0.0487)(4)(96485 \, C \, mol^{-1})(1.8 \, cm^2)(9.33 \times 10^{-3} \, cm^2 \, s^{-1})^{-0.344s}(2.625 \times 10^{-7} \, mol \, cm^{-3})} \right)^3}$$

$D(O_2) = 4.8 \times 10^{-6} cm^2 \, s^{-1}$

Using the experimentally derived value of slope (K), the experimentally determined diffusion coefficient $4.8 \times 10^{-6} cm^2 \, s^{-1}$ for oxygen in ethylene glycol with 3.5% NaCl is computed. However there is no literature available for comparison or oxygen diffusion in ethylene glycol.

3.7.2) Mass transfer coefficient (k$_m$)
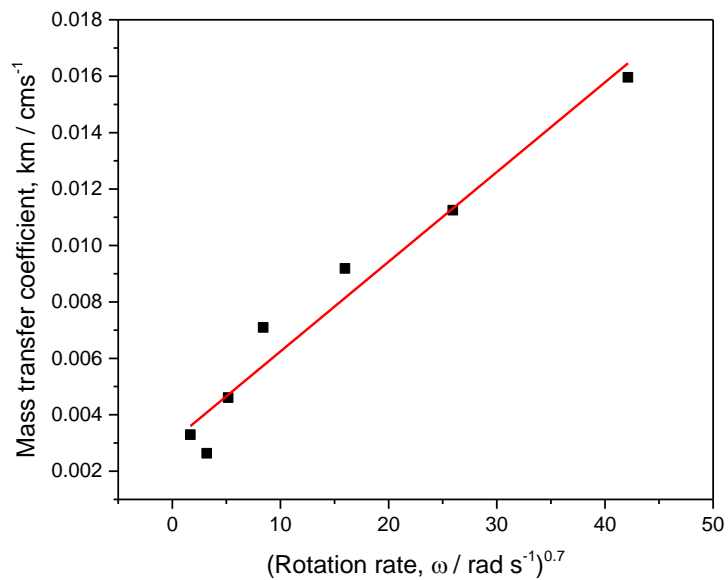
Figure 19: Plots of mass transfer coefficient of oxygen reduction

Mass transfer is the transport of material from bulk of the electrolyte to the surface of electrode or from the surface of electrode to bulk. Limiting current depends on active area of the electrode, A, bulk concentration of dissolved oxygen and mass transport coefficient, k$_m$. Mass transport coefficient is given by equation (10)

$$k_m = \frac{I_L}{zAFC_b}$$

Where z is the number of electrons transferred per oxygen molecule (z=4) and F is the Faraday constant (96485 C mol^{-1}). The mass transport coefficient can be considered as a rate constant that is normalized with respect to dissolved oxygen concentration and cathode area.

Figure4 shows the mass transfer coefficients using the values of diffusion coefficients for oxygen and the mass transfer coefficient *k$_m$* was plotted as a function of

(rotationrate)$^{0.7}$. Mass transfer coefficients of ~0.003 to 0.016 cms^{-1} were calculated. The plot of limiting current against the rotation rate confirms the linear relationship. The mass transfer coefficient values that were obtained in glycol environment are not easy to compare with other hydrodynamic geometries. These values can be related to the higher turbulence intensity that occurs with respect to the rotation rate at which the experiment is carried out which results in enhanced dissolved oxygen mass transfer to the electrode surfaces.

The equations used in part 3.7 were taken from *Study of Mass Transport Limited Corrosion with Rotating Cylinder Electrodes* (18) published by 'Pine research' who manufactured the Rotating Cylinder electrode that was used for this work.

4. Summary

1. The corrosion rate of mild steel in EG depends on the water concentration. Diluted EG is more corrosive than concentrated EG. When chloride is added to the system, the corrosion rate increased.

2. In 100% EG, a protective film was formed on surface of mild steel. When water or NaCl added was added, the film was damaged.

3. Even though iron oxides show catalytic activity on electro-oxidation, we don't have evidences for the oxidation of EG through electrochemistry, since chronoapometry experiment showed negative results. This part has to be done as a separate electrochemistry work.

4. Impedance study corresponds with the results of other electrochemical techniques.

5. Using RCE, flow environment was created and diffusion coefficient of oxygen was calculated.

5. References

1. AlHarooni, K., Pack, D., Iglauer, S., Gubner, R., Ghodkay, V., & Barifcani, A. (2016). Analytical Techniques for Analyzing Thermally Degraded Monoethylene Glycol with Methyl Diethanolamine and Film Formation Corrosion Inhibitor. *Energy & Fuels*, *30*(12), 10937–10949. http://doi.org/10.1021/acs.energyfuels.6b02116

2. Anyadiegwu, C. I. C., Kerunwa, A., & Oviawele, P. (2014). Natural gas dehydration using Triethylene Glycol (TEG). *Petroleum and Coal*, *56*(4), 407–417.

3. Chen, C., Zhu, S., Yang, X., Pi, L., & Cui, Z. (2011). Electro-oxidation of ethylene glycol on nanoporous Ti-Cu amorphous alloy. *Electrochimica Acta*, *56*(27), 10253–10258. http://doi.org/10.1016/j.electacta.2011.09.018

4. Gironi, F., Maschietti, M., & Piemonte, V. (2010). Natural Gas Dehydration: A Triethylene Glycol-Water System Analysis. *Energy Sources, Part A: Recovery, Utilization, and Environmental Effects*, *32*(20), 1861–1868. http://doi.org/10.1080/15567030902804756

5. Gopi, D., Sherif, E. M., Manivannan, V., Rajeswari, D., Surendiran, M., & Kavitha, L. (2014). Corrosion and Corrosion Inhibition of Mild Steel in Groundwater at Di ff erent Temperatures by Newly Synthesized Benzotriazole and Phosphono Derivatives. *Industrial & Engineering Chemistry Research*, *53*, 4286–4294.

6. Khadiri, A., Saddik, R., Bekkouche, K., Aouniti, A., Hammouti, B., Benchat, N., … Solmaz, R. (2015). Gravimetric, electrochemical and quantum chemical studies of some pyridazine derivatives as corrosion inhibitors for mild steel in 1M HCl solution. *Journal of the Taiwan Institute of Chemical Engineers*, *0*, 1–13. http://doi.org/10.1016/j.jtice.2015.06.031

7. Khan, P. F., Shanthi, V., Babu, R. K., Muralidharan, S., & Barik, R. C. (2015). Effect of benzotriazole on corrosion inhibition of copper under flow conditions. *Journal of Environmental Chemical Engineering*, *3*(1), 10–19. http://doi.org/10.1016/j.jece.2014.11.005

8. Kina, A. Y., & Ponciano, J. A. C. (2013). Inhibition of carbon steel CO2 corrosion in

high salinity solutions. *International Journal of Electrochemical Science*, *8*(12), 12600–12612.

9. Kwon, Y., Lai, S. C. S., Rodriguez, P., & Koper, M. T. M. (2011). Electrocatalytic oxidation of alcohols on gold in alkaline media: Base or gold catalysis? *Journal of the American Chemical Society*, *133*(18), 6914–6917. http://doi.org/10.1021/ja200976j

10. Neagu, M., & Cursaru, D. L. (2017). Technical and economic evaluations of the triethylene glycol regeneration processes in natural gas dehydration plants. *Journal of Natural Gas Science and Engineering*, *37*, 327–340. http://doi.org/http://dx.doi.org/10.1016/j.jngse.2016.11.052

11. Rajendran, A., Vinoth, G., Shanthi, V., Barik, R. C., & Pattanayak, D. K. (2014). Silver nano particle incorporated Ti metal prepared by chemical treatment for antibacterial and corrosion resistance study. *Orthopaedic Biomaterials*, *29*. http://doi.org/10.1179/1753555713Y.0000000113

12. Santambrogio, M., Perrucci, G., Trueba, M., Trasatti, S. P., & Casaletto, M. P. (2015). Effect of major degradation products of ethylene glycol aqueous solutions on steel corrosion. *Electrochimica Acta*, (2015), 1–12. http://doi.org/10.1016/j.electacta.2016.03.144

13. Schwerdtfeger, W. J. (1957). Measurement of the corrosion rate of iron by polarization techniques. *Journal of Research of the National Bureau of Standards*, *58*(3), 145–153. http://doi.org/10.6028/jres.058.020

14. Sekine, I., Hayakawa, T., Negishi, T., & Yuasa, M. (1990). Analysis for corrosion behavior of mild steels in various hydroxy acid solutions by new methods of surface analyses and electrochemical measurements. *Journal of the Electrochemical Society*, *137*(10), 3029–3033. http://doi.org/10.1149/1.2086153

15. Sekunowo, O. I., Adeosun, S. O., & Lawal, G. I. (2013). Potentiostatic Polarisation Responses Of Mild Steel In Seawater And Acid Environments. *International Journal of Scientific & Technology Research*, *2*(10), 139–145.

16. Silverman, D. C., & Carrico, J. E. (1988). Electrochemical Impedance Technique - a Practical Tool for Corrosion Prediction. *Corrosion*, *44*(5), 280–287. http://doi.org/10.5006/1.3583938

17. Xin, L., Zhang, Z., Qi, J., Chadderdon, D., & Li, W. (2012). Electrocatalytic oxidation of ethylene glycol (EG) on supported Pt and Au catalysts in alkaline media: Reaction pathway investigation in three-electrode cell and fuel cell reactors. *Applied Catalysis B: Environmental*, *125*, 85–94. http://doi.org/10.1016/j.apcatb.2012.05.024

18. https://www.pineresearch.com/shop/wp-content/uploads/sites/2/2016/07/DRA10011-Study-of-Mass-Transport-Limited-Corrosion-with-Rotating-Cylinder-Electrodes-REV003.pdf